

**NASA TECHNICAL NOTE**



**NASA TN D-5278**

C.1

**NASA TN D-5278**

OFF COPY: RE-FILED  
FILE (WHL-2)  
KIRTLAND AFB, N M

0132250



**TECH LIBRARY KAFB, NM**

# EXPLORATORY STUDY OF OPEN-FACE HONEYCOMB TO REDUCE TEMPERATURE OF HYPERSONIC AIRCRAFT STRUCTURE

*by L. Roane Hunt and R. R. Howell*

*Langley Research Center*

*Langley Station, Hampton, Va.*



0132250

1. Report No. NASA TN D-5278		2. Government Accession No.		3. Recipient's Catalog No.	
4. Title and Subtitle EXPLORATORY STUDY OF OPEN-FACE HONEYCOMB TO REDUCE TEMPERATURE OF HYPERSONIC AIRCRAFT STRUCTURE		5. Report Date June 1969		6. Performing Organization Code	
		8. Performing Organization Report No. L-6383		10. Work Unit No. 126-13-03-47-23	
7. Author(s) L. Roane Hunt and R. R. Howell		11. Contract or Grant No.		13. Type of Report and Period Covered Technical Note	
9. Performing Organization Name and Address NASA Langley Research Center Langley Station Hampton, Va. 23365		14. Sponsoring Agency Code			
12. Sponsoring Agency Name and Address					
15. Supplementary Notes					
16. Abstract  An exploratory study was conducted in the Langley 7-inch Mach 7 pilot tunnel to determine the effectiveness of open-face honeycomb structure as a means of reducing the temperature of a hypersonic aircraft structure. The wind-tunnel tests were conducted at a unit Reynolds number of $9 \times 10^5$ per foot ( $3 \times 10^6$ per meter), a Mach number of 7.0, a stagnation temperature of $3400^\circ \text{R}$ ( $1890^\circ \text{K}$ ), and angles of attack from $0^\circ$ to $10^\circ$ . The results indicate that for zero angle of attack the steady-state temperatures of the surfaces beneath open-face honeycomb structure were 0.82 to 0.88 of a smooth reference surface under the same conditions.					
17. Key Words Suggested by Author(s) Open-face honeycomb Surface structural concept Heat shield Hypersonic aircraft Steady-state temperature			18. Distribution Statement  Unclassified - Unlimited		
19. Security Classif. (of this report) Unclassified	20. Security Classif. (of this page) Unclassified	21. No. of Pages 23	22. Price* \$3.00		

\*For sale by the Clearinghouse for Federal Scientific and Technical Information  
Springfield, Virginia 22151

# EXPLORATORY STUDY OF OPEN-FACE HONEYCOMB TO REDUCE TEMPERATURE OF HYPERSONIC AIRCRAFT STRUCTURE

By L. Roane Hunt and R. R. Howell  
Langley Research Center

## SUMMARY

An exploratory study was conducted in the Langley 7-inch Mach 7 pilot tunnel to determine the effectiveness of open-face honeycomb structure as a means of reducing the temperature of a hypersonic aircraft structure. The wind-tunnel tests were conducted at a unit Reynolds number of  $9 \times 10^5$  per foot ( $3 \times 10^6$  per meter), a Mach number of 7.0, a stagnation temperature of  $3400^\circ \text{R}$  ( $1890^\circ \text{K}$ ), and angles of attack from  $0^\circ$  to  $10^\circ$ . The results indicate that for zero angle of attack the steady-state temperatures of the surfaces beneath open-face honeycomb structure were 0.82 to 0.88 of a smooth reference surface temperature, and the maximum temperature at the outer edge of the honeycomb structure was equal to or less than that of the reference surface. The advantage of the open-face honeycomb structure decreased with increase in angle of attack, increase in honeycomb cell width, and reduction in cell depth.

## INTRODUCTION

One of the many problems facing the designer of hypersonic vehicles is that of controlling the structural temperature without excessive weight or performance penalty. Excessive temperature and temperature differences within the structure are reflected in weight increases to avoid intolerable stress levels and deflections. Consequently, it is desirable to devise efficient methods of controlling the temperature of the structure. A new surface concept, considered herein, is the use of open-faced honeycomb cells attached to the outer surface of a conventional skin as a possible means of reducing the temperature of the substructure. When the honeycomb cells are washed by the stream, the surface area in contact with the stream is small in comparison with that of a plane surface, and the aerodynamic heating is limited to flow impingement on the cell surface near the stream and to flow circulation within the cell. Theoretical and experimental results of references 1 and 2 indicate that the aerodynamic heating of separated flow, such as that in the honeycomb cell, is about 0.6 of that of attached flow. The exposed cellular structure also improves the emission characteristics of the surface (see ref. 3)

so that increased radiation is achieved with a resulting reduction in the temperature of the substructure.

This paper presents the results of an experimental study conducted in the Langley 7-inch Mach 7 pilot tunnel to determine the effectiveness of the open-face honeycomb structure as a means of reducing the steady-state temperature of a surface. Honeycomb panels of various cell widths and depths were tested at a unit Reynolds number of  $9 \times 10^5$  per foot ( $3 \times 10^6$  per meter), a Mach number of 7.0, and a stagnation temperature of  $3400^\circ \text{R}$  ( $1890^\circ \text{K}$ ). Panel steady-state temperatures were determined for angles of attack from  $0^\circ$  to  $10^\circ$ .

### SYMBOLS

The units used for the physical quantities in this paper are given both in the U.S. Customary Units and in the International System of Units (SI). Factors relating the two systems are given in reference 4, and those used in the present investigation are presented in the appendix.

d	honeycomb cell depth, in. (m)
h	convective heat-transfer coefficient, $\text{Btu}/\text{ft}^2\text{-sec-}^\circ\text{R}$ ( $\text{W}/\text{m}^2\text{-}^\circ\text{K}$ )
$N_{\text{Re}}$	Reynolds number
R	thermal resistance, $\text{ft}^2\text{-sec-}^\circ\text{R}/\text{Btu}$ ( $\text{m}^2\text{-}^\circ\text{K}/\text{W}$ )
$R_e$	thermal resistance of panel A, $\text{ft}^2\text{-sec-}^\circ\text{R}/\text{Btu}$ ( $\text{m}^2\text{-}^\circ\text{K}/\text{W}$ )
$R_t$	thermal resistance of present test, $\text{ft}^2\text{-sec-}^\circ\text{R}/\text{Btu}$ ( $\text{m}^2\text{-}^\circ\text{K}/\text{W}$ )
r	radius, in. (m)
T	temperature, $^\circ\text{R}$ ( $^\circ\text{K}$ )
w	honeycomb cell width, in. (m)
x	longitudinal distance from leading edge of panel holder, in. (m)
y	lateral distance from center line of panel holder, in. (m)

$\alpha$	angle of attack of panel to stream (see fig. 1), deg
$\delta$	boundary-layer thickness, in. (m)
$\epsilon$	surface emissivity
$\sigma$	Stefan-Boltzmann constant, Btu/ft <sup>2</sup> -sec-°R <sup>4</sup> (W/m <sup>2</sup> -°K <sup>4</sup> )

#### Subscripts:

a	ambient condition
aw	laminar adiabatic wall
i	inner face sheet
m	midpoint of cell depth
o	outer edge or outer face sheet
r	reference value

## APPARATUS AND TESTS

### Panels

Four honeycomb sandwich panels were aerothermodynamically tested in the Langley 7-inch Mach 7 pilot tunnel. One of the panels was a conventional closed-face honeycomb sandwich and is hereinafter referred to as the sandwich honeycomb panel or panel A. The other three panels were open-face honeycomb sandwich obtained by removing the outer face sheet. These panels are referred to herein as open-face honeycomb panels or panels B, C, and D. The panels were fabricated of stainless steel with a square cell core brazed to the face sheets. The test area of the panels was 3.0 inches (7.6 cm) wide and 3.6 inches (9.1 cm) long. Cell widths of 3/16 and 1/8 inch (4.8 and 3.2 mm) were tested with depths varying between 0.38 and 0.64 inch (9.7 and 16.3 mm). Pertinent panel details are presented as table I.

The panels were mounted for testing in a flat-plate panel holder which has a width of 4.0 inches (10.2 cm) and a leading-edge radius of 0.03 inch (0.76 mm). A sketch and photographs of the panel assembly are presented as figures 1 and 2, respectively. The panels were secured in the panel holder by peripheral clamping of an extended portion of the inner face sheet of each panel. The clamping was accomplished with uncured cast

silica blocks, the dimensions of which were such as to bring the outer panel edge flush with the top surface of the holder. (See detail A of fig. 1.) Quartz-felt insulation was packed against the bottom of the panels to minimize the heat leakage from the panels.

All panels were instrumented with chromel-alumel thermocouples in the manner indicated in detail B of figure 1. Three thermocouple positions were used: position o, on the backside of the outer face sheet for panel A and within 0.05 inch (1.3 mm) of the outer edge for the open-face honeycomb; position m, at the midpoint of the cell depth; and position i, on the bottom surface of the inner face sheet. The longitudinal and lateral locations of each thermocouple are presented in table II.

### Facility

The tests were conducted in the Langley 7-inch Mach 7 pilot tunnel. The facility is a hypersonic blowdown tunnel with a high energy level obtained by burning a mixture of methane and air under pressure. Air, introduced at pressures up to 2300 psi (16 MN/m<sup>2</sup>), is mixed with methane and burned in the combustion chamber. The combustion gases are then expanded to a nominal Mach number of 7.0 by use of the axisymmetric contoured nozzle. The gases flow through the free-jet test section and straight tube diffuser into the single-stage air ejector which pumps the mixture into the atmosphere. The stagnation temperature is a function of the air-fuel ratio which was controlled.

Diametrical pitot-pressure and stagnation-temperature surveys made over the length of the test region indicate a usable test-core diameter of about 3.0 inches (7.6 cm). Within the test core there is a  $\pm 2$ -percent variation of total temperature. Previous studies (refs. 5 and 6) indicate that the aerodynamic heating and loading coefficients obtained in the combustion-products test medium of this facility are comparable to those obtained in air-test facilities.

The output of thermocouples and transducers monitoring the tunnel conditions and temperatures on the panels were recorded with a digital recording system sampling at a rate of 20 times per second. These data, reduced to temperatures and pressures, were used to determine tunnel test conditions and the panel temperatures. The thermodynamic, transport, and flow properties of the gas used in the reduction of the present data were determined by the methods discussed in reference 7.

### Tests

All tests were made at a stagnation temperature of 3400° R (1890° K), a dynamic pressure of 5.0 psi (34 kN/m<sup>2</sup>), a nominal Mach number of 7.0, and a unit Reynolds number of  $9 \times 10^5$  per foot ( $3 \times 10^6$  per meter). In general, the panels were tested over a range of angles of attack  $\alpha$  from 0° to 10°. However, panel C was limited to angles

of attack of  $0^\circ$  and  $2^\circ$  as a result of warpage. The manner in which the panels were supported caused thermal stress levels within the panels, and these stress levels caused the panels to warp with successive thermal cycling. After two cycles the deformation became excessive for panel C, and the panel could no longer be tested.

The test procedure was to establish the desired test conditions in the tunnel and then to insert the model into the test region. At low angles of attack, panel steady-state temperatures could not be reached within the 2 or 3 minutes of tunnel test time. To achieve steady-state temperature within a reasonable test period, the panels were inserted at an angle to the flow greater than the test angle. This procedure increased the heating rate and consequently the temperature rise rate. When the temperatures were near the expected steady-state value, the panels were pitched to the lower, predetermined test angle where temperatures adjusted to the steady-state value.

## RESULTS AND DISCUSSION

### Panel Temperature

Steady-state temperatures were determined from thermocouple outputs after several minutes of testing in a constant environment and after the outputs had reached a near-zero rate of change. The ratio of the panel temperature  $T$  to the laminar, free-stream, adiabatic wall temperature  $T_{aw}$  is presented in figures 3 and 4. The nominal value of  $T_{aw}$  for the present test was  $3000^\circ \text{ R}$  ( $1670^\circ \text{ K}$ ) with a maximum variation of  $\pm 100^\circ \text{ R}$  ( $56^\circ \text{ K}$ ).

The longitudinal and lateral temperature distributions for the three thermocouple positions of the honeycomb panels at  $\alpha = 0^\circ$  are presented as figure 3. The temperature gradient along the inner face sheets indicated heat leakage to the panel holder. Consequently, a location near the center of the panels at  $x = 5$  inches (12.7 cm),  $y = 0$  was selected as the location for the data comparisons and performance evaluation.

The panel temperatures referenced to adiabatic wall temperature for positions o and i are presented as a function of angle of attack in figure 4. All the data from the present study are summarized by this figure. The increase in panel temperature with angle of attack is indicative of the increase in convective heating to a surface with angle of attack.

### Reference Temperature

To determine the possible advantage of the open-face honeycomb as a thermal protection device, it was necessary to compare the steady-state temperature of the open-face honeycomb panel face sheet with the temperature of a smooth surface without the

honeycomb present. Ideally, this reference temperature should be determined experimentally by subjecting a smooth, properly supported, and insulated surface to the same environment used for the open-face honeycomb panel tests. The practical problems of keeping a thin, metal surface flat while testing to steady-state temperature, however, precluded this approach. As the best alternative a sandwich honeycomb panel (panel A) was tested. While this approach permitted the use of the honeycomb core to keep the surface flat, it had the possible modifying effect of lacking the correct surface insulation. Calculations were subsequently made to determine the expected difference between the desired reference temperature and the surface temperature of panel A for various panel insulation levels. In making these calculations, one-dimensional steady-state heat flow was assumed. The heat-balance equations used were as follows:

$$h(T_{aw} - T_o) - \sigma \epsilon T_o^4 - \frac{1}{R_e}(T_o - T_i) = 0 \quad (1)$$

$$\frac{1}{R_e}(T_o - T_i) - \frac{1}{R}(T_i - T_a) = 0 \quad (2)$$

where the symbols are as defined in the symbol list and by the sketch in figure 5. The convective heat-transfer coefficient  $h$  was determined from experimental transient-heat-transfer data and was substantiated by theoretical computations. Also, the thermal resistance  $R_e$  of panel A was determined from experimental transient-temperature data and substantiated by calculations using the method discussed in reference 8. With the use of the test values of  $T_{aw}$ ,  $T_o$ , and  $T_i$ , the panel surface emissivity  $\epsilon$  was computed to be 0.51 from equation (1) and the thermal resistance of the insulation beneath the panels during the present tests  $R_t$  was found to be 5000 ft<sup>2</sup>-sec-°R/Btu (0.245 m<sup>2</sup>-°K/W) from equation (2).

The results of the computation are presented as figure 5. The ratio of the wall temperature  $T$  to the adiabatic wall temperature  $T_{aw}$  is presented as a function of the ratio of the resistance  $R$  to the test resistance  $R_t$ . The desired reference temperature  $T_r$  corresponds to a properly insulated smooth surface. The experimental temperatures  $T_o/T_{aw}$  and  $T_i/T_{aw}$  plotted at  $R/R_t = 1$  agree with the computed curves as dictated by the computation procedure indicated earlier. For the test resistance, the difference between  $T_o/T_{aw}$  and  $T_r/T_{aw}$  is insignificant, and the steady-state temperature is 97 percent of the radiation equilibrium value. It was concluded that the measured steady-state surface temperature of panel A should be an accurate representation of the corresponding temperature of a smooth surface and could be used as a reference in the evaluation of the honeycomb panel. This reference temperature was designated as  $T_r$ .



## Thermal Performance of the Open-Face Honeycomb Panels

Inner-face-sheet temperature.- The ratio of the inner-face-sheet temperature (position i) of the open-face honeycomb panels (panels B, C, and D) to the reference temperature is presented as a function of  $\alpha$  in figure 6. (See diamond-shape test-point symbols.) At  $\alpha = 0^\circ$ , the temperature of the face sheet of the open-face honeycomb panels was significantly less than the reference temperature. The values of  $T/T_r$  were 0.88 for panels B and C and 0.82 for panel D. Reducing the depth of the honeycomb cell from 0.64 to 0.38 inch (16.3 to 9.7 mm) did not change the face-sheet temperature at  $\alpha = 0^\circ$ . (Compare panel B results with panel C results.) Reducing the cell depth did, however, increase the sensitivity of the panel to angle of attack. Reducing the cell width from 3/16 to 1/8 inch (4.8 to 3.2 mm) reduced both the face-sheet temperature and the sensitivity of the panel to angle of attack. (Compare panel B results with panel D results.) The face-sheet temperature approached the reference temperature with increase in angle of attack, and  $T/T_r$  for panel B exceeded unity at  $\alpha = 9^\circ$ . This trend with angle of attack cannot be fully explained in the present study; however, local values of Mach number, pressure, and boundary-layer thickness, which are functions of angle of attack, could be factors causing the increased temperature.

Outer-edge temperature.- The cell outer-edge temperatures (position o) for the open-face honeycomb panels are indicated by the circular symbols in figure 6. It is important to note that the temperatures are generally equal to or less than the corresponding reference temperatures. Therefore, the material constraints for the open-face honeycomb concept appear to be no more severe than those of the insulated wall (or conventional skin).

Boundary-layer thickness effect.- In the present study of open-face honeycomb panels with thin laminar boundary layers, the ratio of the boundary-layer thickness  $\delta$  to the honeycomb cell width  $w$  appears to be an important parameter in correlating the performance of the open-face honeycomb. This parameter is also suggested for individual cavities by references 9 and 10. The face-sheet temperature ratio for panels B and D, which have comparable cell width-to-depth ratios  $w/d$  of 0.29 and 0.25, is presented as a function of  $\delta/w$  in figure 7. The boundary-layer thickness varied with angle of attack and was computed from the following equation from reference 11:

$$\delta = \frac{5x}{\sqrt{N_{Re}}}$$

Figure 7 indicates that the thermal performance of the open-face honeycomb panels improves with increase in boundary-layer thickness. Also, the open-face honeycomb is most effective as thermal protection when the boundary-layer thickness is greater than about 0.6 of the cell width.

### Thermal-Performance Index

An index of thermal performance of a surface can be obtained from the heat-balance equation of a perfectly insulated surface as follows:

$$\frac{h}{\epsilon} = \frac{\sigma T^4}{T_{aw} - T} \quad (3)$$

Since  $T_{aw}$  is defined by stream conditions, the surface temperature is determined by the heat-transfer coefficient  $h$  and the surface emissivity  $\epsilon$ . Consequently, changes in temperature that result from different surface conditions may reflect changes in either  $h$  or  $\epsilon$ , or both. Therefore, the ratio of  $h/\epsilon$  is an index of thermal performance for highly insulated surfaces and should be a useful index for the present results.

The ratio of  $h/\epsilon$  for the face sheet of the open-face honeycomb to that of the reference surface  $\frac{h/\epsilon}{(h/\epsilon)_r}$  is presented as a function of  $\alpha$  in figure 8. At  $\alpha = 0^\circ$  it is indicated that the presence of the honeycomb reduces the effective value of  $h/\epsilon$  to 0.49, 0.45, and 0.35 of the reference value for panels B, C, and D, respectively. Inasmuch as  $h/\epsilon$  and  $T^4$  are related through equation (3), the trends of  $h/\epsilon$  with cell width, cell depth, and  $\alpha$  are similar to those of temperature in figure 6. The trends of  $h/\epsilon$  are, however, magnified because of the exponent of  $T$ . Consequently, the advantages of the open-face honeycomb panels are indicated more clearly when presented in terms of  $h/\epsilon$ .

### Concept Application

An application for the cellular surface concept as thermal protection seems apparent when the temperature limits for the structural material and the steady-state temperature are compatible. Under this constraint the concept could be applied as an effective means of reducing the working temperature of the support structure. Cell depth and width appear to be possible controls for the support-structure working-temperature distribution. However, before the concept can be applied to aircraft, additional factors must be considered. For example, additional studies are required to establish the performance of open-face honeycomb surfaces with thick turbulent boundary layers. The skin-friction force and pressure drag produced by hypersonic flow over open-face honeycomb also remains to be evaluated. A theoretical analysis by Chapman (ref. 1) indicates that skin friction of laminar separated flow, such as produced in the honeycomb cells, is about 0.6 of the laminar attached flow. Reynolds' analogy, which relates the skin friction to the heat transfer, supports the conclusion of Chapman's analysis. Therefore, if the pressure drag increment associated with the effective roughness of the honeycomb is small, the concept can be applied with little loss in aerodynamic performance.

## CONCLUDING REMARKS

An exploratory study has been conducted in the Langley 7-inch Mach 7 pilot tunnel to determine the thermal performance of open-face honeycomb sandwich panels, and the results are compared with the performance of a smooth reference surface. The tunnel tests were conducted at a unit Reynolds number of  $9 \times 10^5$  per foot ( $3 \times 10^6$  per meter), a Mach number of 7.0, a stagnation temperature of  $3400^\circ \text{R}$  ( $1890^\circ \text{K}$ ), and angles of attack from  $0^\circ$  to  $10^\circ$ .

The results of the study indicated that for zero angle of attack the steady-state temperatures of surfaces beneath the open-face honeycomb were 0.82 to 0.88 of a smooth reference surface temperature, and the maximum temperature at the outer edge of the honeycomb was equal to or less than that of a reference surface. The advantage of the open-face honeycomb decreased with increase in angle of attack, increase in honeycomb cell width, and reduction in cell depth. Additional studies are needed to evaluate more fully this approach to the reduction of aerodynamic heating.

Langley Research Center,  
National Aeronautics and Space Administration,  
Langley Station, Hampton, Va., April 8, 1969,  
126-13-03-47-23.

## APPENDIX

### CONVERSION OF U.S. CUSTOMARY UNITS TO SI UNITS

Factors required for converting the units used herein to the International System of Units (SI) are given in the following table:

Physical quantity	U.S. Customary Unit	Conversion factor (*)	SI unit (**)
Heat-transfer coefficient . . . .	Btu/ft <sup>2</sup> -sec-°R	$2.042 \times 10^4$	watts/meter <sup>2</sup> -degree Kelvin (W/m <sup>2</sup> -°K)
Length . . . . .	in.	0.0254	meters (m)
	per ft	3.28	per meter (m <sup>-1</sup> )
Pressure . . . . .	psi	$6.895 \times 10^3$	newtons/meter <sup>2</sup> (N/m <sup>2</sup> )
Temperature . . . . .	°R	5/9	degrees Kelvin (°K)
Thermal resistance . . . . .	ft <sup>2</sup> -sec-°R/Btu	$4.90 \times 10^{-5}$	meter <sup>2</sup> -degrees Kelvin/watt (m <sup>2</sup> -°K/W)
Stefan-Boltzmann constant . . .	Btu/ft <sup>2</sup> -sec-°R <sup>4</sup>	$1.1915 \times 10^5$	watts/meter <sup>2</sup> -degree Kelvin <sup>4</sup> (W/m <sup>2</sup> -°K <sup>4</sup> )

\*Multiply value in U.S. Customary Unit by conversion factor to obtain equivalent value in SI unit.

\*\*Prefixes to indicate multiples of units are as follows:

Prefix	Multiple
mega (M)	10 <sup>6</sup>
kilo (k)	10 <sup>3</sup>
centi (c)	10 <sup>-2</sup>
milli (m)	10 <sup>-3</sup>

## REFERENCES

1. Chapman, Dean R.: A Theoretical Analysis of Heat Transfer in Regions of Separated Flow. NACA TN 3792, 1956.
2. Larson, Howard K.: Heat Transfer in Separated Flows. J. Aero/Space Sci., vol. 26, no. 11, Nov. 1959, pp. 731-738.
3. Sparrow, E. M.: Radiant Emission Characteristics of Nonisothermal Cylindrical Cavities. Appl. Opt., vol. 4, no. 1, Jan. 1965, pp. 41-43.
4. Comm. on Metric Pract.: ASTM Metric Practice Guide. NBS Handbook 102, U.S. Dep. Com., Mar. 10, 1967.
5. Weinstein, Irving: Heat Transfer and Pressure Distributions on a Hemisphere-Cylinder and a Bluff-Afterbody Model in Methane-Air Combustion Products and in Air. NASA TN D-1503, 1962.
6. Hunt, L. Roane: Aerodynamic Force and Moment Characteristics of Spheres and Cones at Mach 7.0 in Methane-Air Combustion Products. NASA TN D-2801, 1965.
7. Leyhe, E. W.; and Howell, R. R.: Calculation Procedure for Thermodynamic, Transport, and Flow Properties of the Combustion Products of a Hydrocarbon Fuel Mixture Burned in Air With Results for Ethylene-Air and Methane-Air Mixtures. NASA TN D-914, 1962.
8. Swann, Robert T.; and Pittman, Claud M.: Analysis of Effective Thermal Conductivities of Honeycomb-Core and Corrugated-Core Sandwich Panels. NASA TN D-714, 1961.
9. Nestler, D. E.; Saydah, A. R.; and Auxer, W. L.: Heat Transfer to Steps and Cavities in Hypersonic Turbulent Flow. AIAA Paper No. 68-673, June 1968.
10. Dhanak, A. M.: Heat Transfer and Drag Due to Cavities on a Re-Entry Surface. Problems of Propulsion and Re-Entry, P. Contensou, G. N. Duboshin, and W. F. Hilton, eds., Gordon and Breach, Inc., 1967, pp. 403-409.
11. Schlichting, Hermann (J. Kestin, trans.): Boundary-Layer Theory. Sixth ed., McGraw-Hill Book Co., 1968.

TABLE I.- PERTINENT PANEL DETAILS

Panel	Cell depth		Cell width		Cell wall thickness		Face sheet thickness	
	in.	mm	in.	mm	in.	mm	in.	mm
A	0.48	12.2	3/16	4.8	0.0015	0.038	0.010	0.25
B	.64	16.3	3/16	4.8	.0015	.038	.010	.25
C	.38	9.7	3/16	4.8	.0015	.038	.010	.25
D	.50	12.7	1/8	3.2	.0020	.051	.023	.58

TABLE II.- LONGITUDINAL AND LATERAL LOCATIONS  
OF PANEL THERMOCOUPLES

(a) U.S. Customary Units

Panel A		Panel B		Panel C		Panel D	
x, in.	y, in.	x, in.	y, in.	x, in.	y, in.	x, in.	y, in.
Thermocouple position o (within 0.05 in. of outer edge)							
5.00	0.45	4.05	-0.20	4.80	-0.20	4.00	-0.45
		4.25	-.40	4.95	.10	3.95	-.45
		5.15	-.05	5.20	.20	4.90	-.40
		5.55	-.20			4.75	-.40
		6.55	0			6.30	-.60
		6.55	-.40			6.40	.50
						6.45	-.55
						6.30	.40
Thermocouple position m (midpoint of cell depth)							
		4.35	-0.25				
		4.45	-.40				
		5.15	-.35				
		5.35	-.05				
		6.20	-.10				
		6.70	-.20				
Thermocouple position i (bottom of inner face sheet)							
4.0	-0.30	4.35	0.15	4.10	-0.30	4.00	-1.20
4.0	.20	4.25	0	3.95	0	4.00	-.45
5.0	-.45	5.20	.35	5.15	-.30	4.05	.50
5.2	-.10	5.50	.25	5.25	-.10	5.05	-.40
5.0	-.05	4.95	.15	5.00	-.30	5.05	.40
5.0	.20	5.05	.35	5.00	.30	4.90	-.20
5.32	.30	5.30	.15	5.10	.30	4.85	.35
5.22	.05	5.60	.05	5.10	.10	5.15	.50
6.60	-.15	6.60	.20	6.50	-.15	6.50	-.60
6.70	-.25	6.65	.30	6.65	.10	6.15	-.60
6.45	.10			5.00	-1.20		
6.45	.20			5.00	1.20		
4.00	-.20						
4.00	.10						

TABLE II.- LONGITUDINAL AND LATERAL LOCATIONS  
OF PANEL THERMOCOUPLES - Concluded

(b) SI units

Panel A		Panel B		Panel C		Panel D	
x, cm	y, cm	x, cm	y, cm	x, cm	y, cm	x, cm	y, cm
Thermocouple position o (within 0.05 in. of outer edge)							
12.7	1.14	10.3	-0.51	12.2	-0.51	10.2	-1.14
		10.8	-1.02	12.6	.25	10.0	-1.14
		13.1	-.13	13.2	.51	12.4	-1.02
		14.1	-.51			12.6	-1.02
		16.6	0			16.0	-1.52
		16.6	-1.02			16.3	1.27
						16.4	-1.40
						16.0	1.02
Thermocouple position m (midpoint of cell depth)							
		11.0	-0.64				
		11.3	-1.02				
		13.1	-.89				
		13.6	-.13				
		15.7	-.25				
		17.0	-.51				
Thermocouple position i (bottom of inner face sheet)							
10.2	-0.76	11.0	0.38	10.4	-0.76	10.2	-3.05
10.2	.51	10.8	0	10.0	0	10.2	-1.14
12.7	-1.14	13.2	.89	13.1	-.76	10.3	1.27
13.2	-.25	14.0	.63	13.3	-.25	12.8	-1.02
12.7	-.13	12.6	.38	12.7	-.76	12.8	1.02
12.7	.51	12.8	.89	12.7	.76	12.4	-.51
13.5	.76	13.5	.38	13.0	.76	12.3	.89
13.3	.13	14.2	.13	13.0	.25	13.1	1.27
16.7	-.38	16.8	.51	16.5	-.38	16.5	-1.52
17.0	-.63	16.9	.76	16.9	.25	15.6	-1.52
16.4	.25			12.7	-3.05		
16.4	.51			12.7	3.05		
10.2	-.51						
10.2	.25						



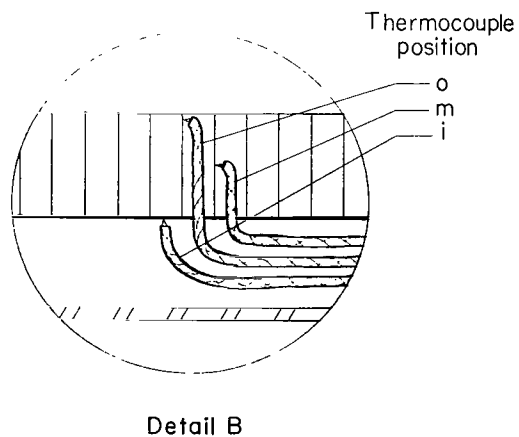
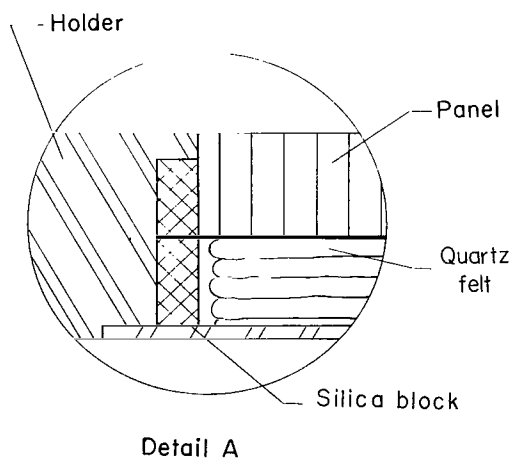
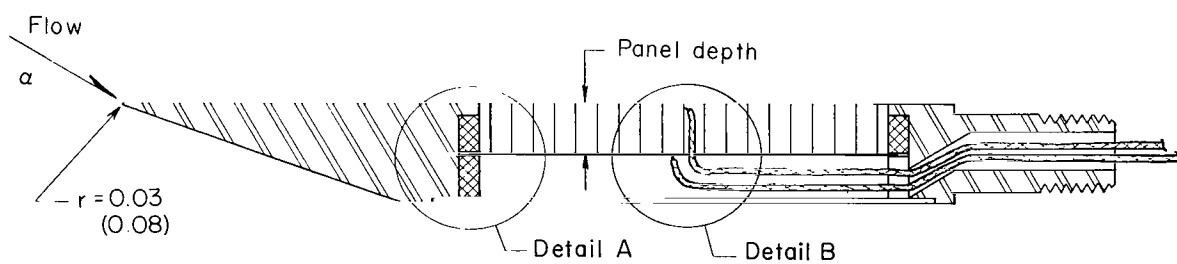
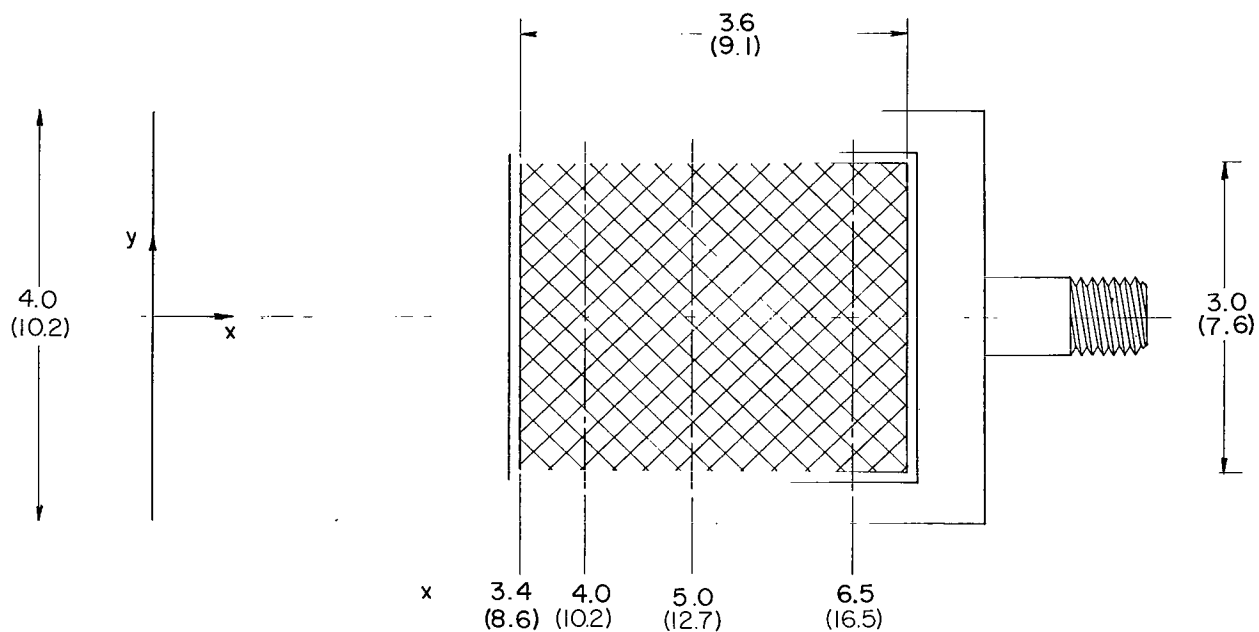
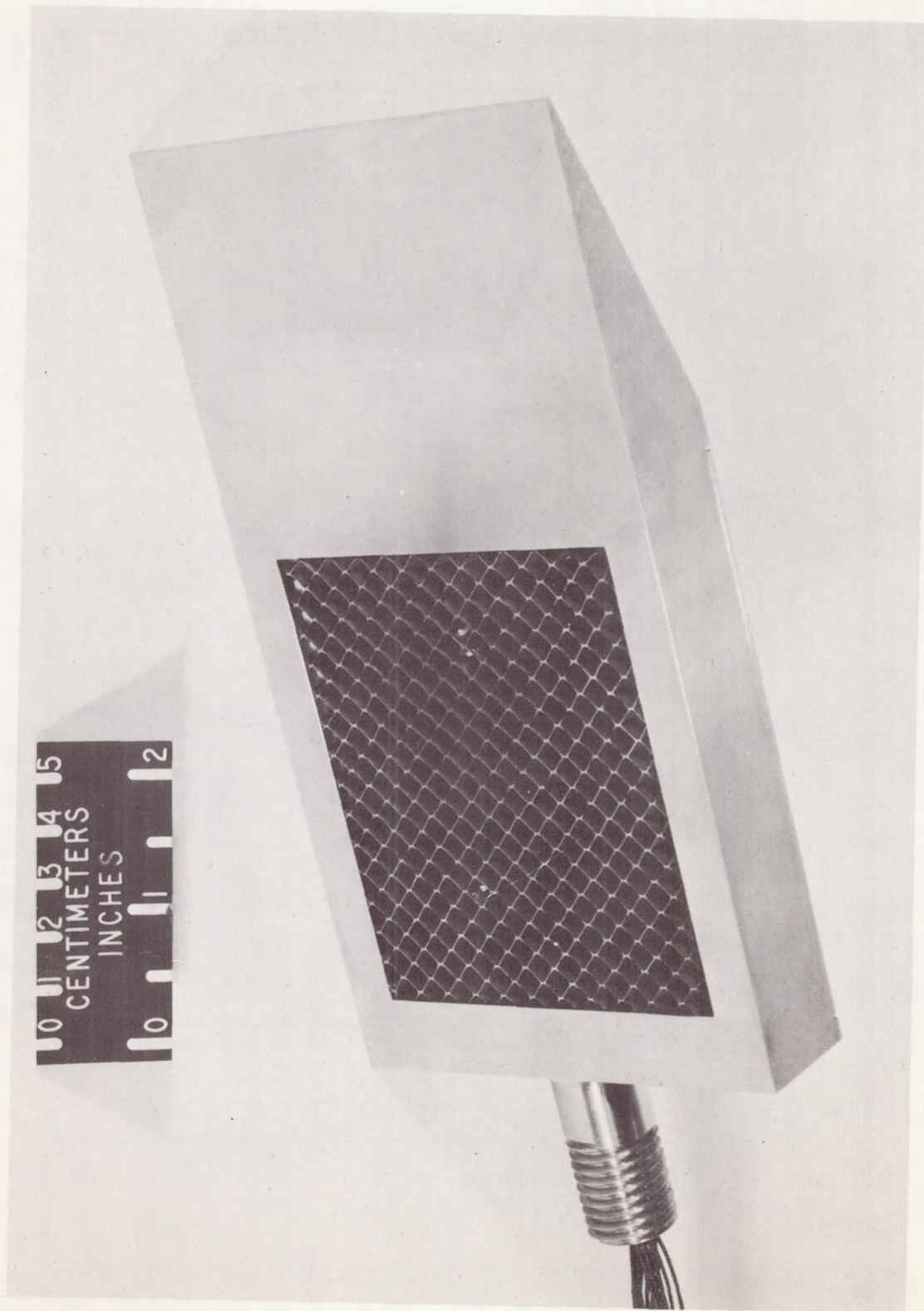


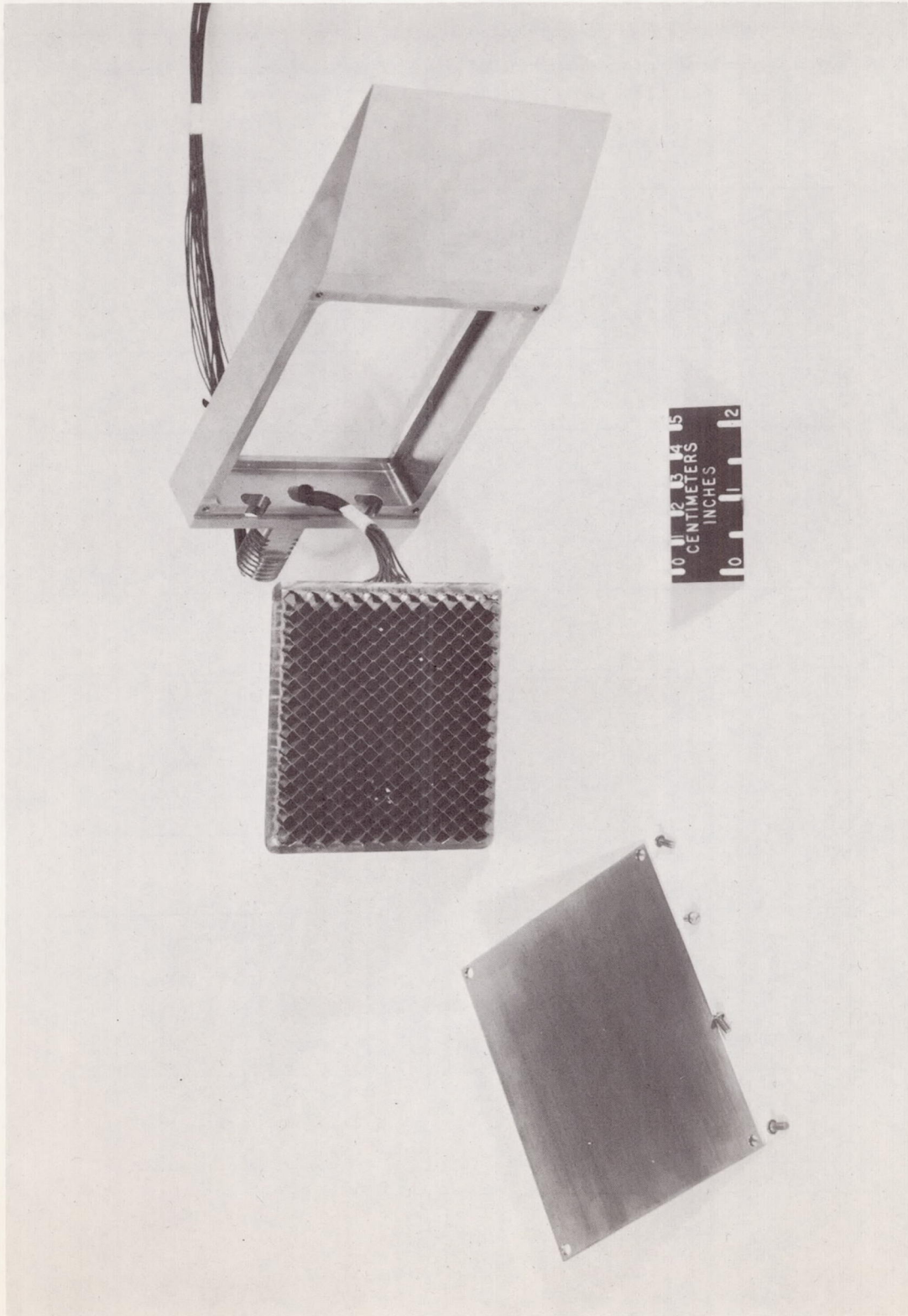
Figure 1.- Sketch of panel assembly. (All dimensions given first in inches and parenthetically in centimeters.)



(a) Assembly.

L-66-6534

Figure 2.- Photographs of panel and holder.



(b) Disassembly.

Figure 2.- Concluded.

L-66-6533

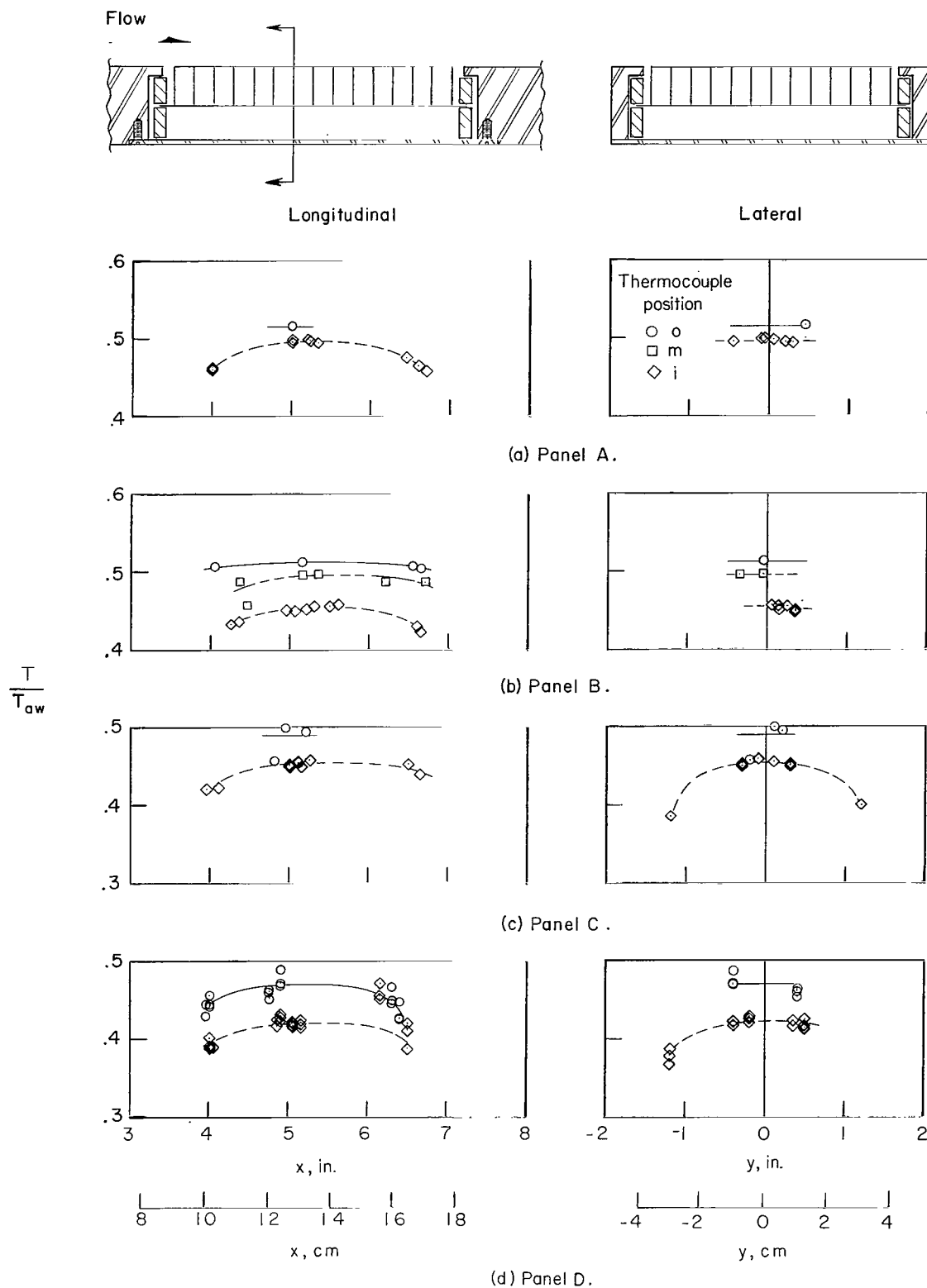


Figure 3.- Temperature distributions of panels tested at zero angle of attack.  $T_{\infty} = 3000^{\circ} \text{ R}$  ( $1670^{\circ} \text{ K}$ ).

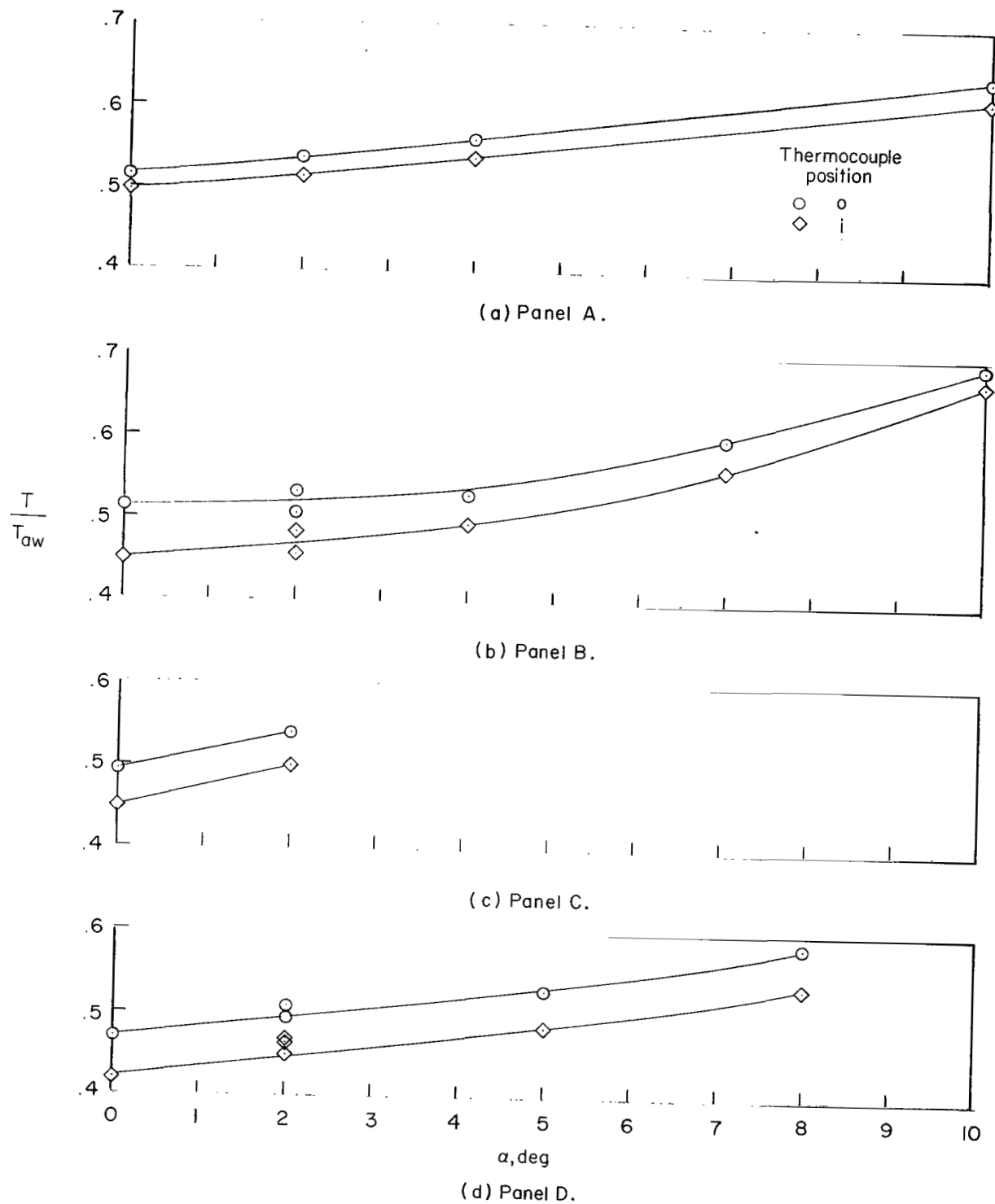


Figure 4.- Variation of  $T/T_{aw}$  for inner and outer surfaces of panels with angle of attack.  
 $x = 5$  inches (12.7 cm);  $y = 0$ ;  $T_{aw} = 3000^\circ \text{R}$  (1670° K).

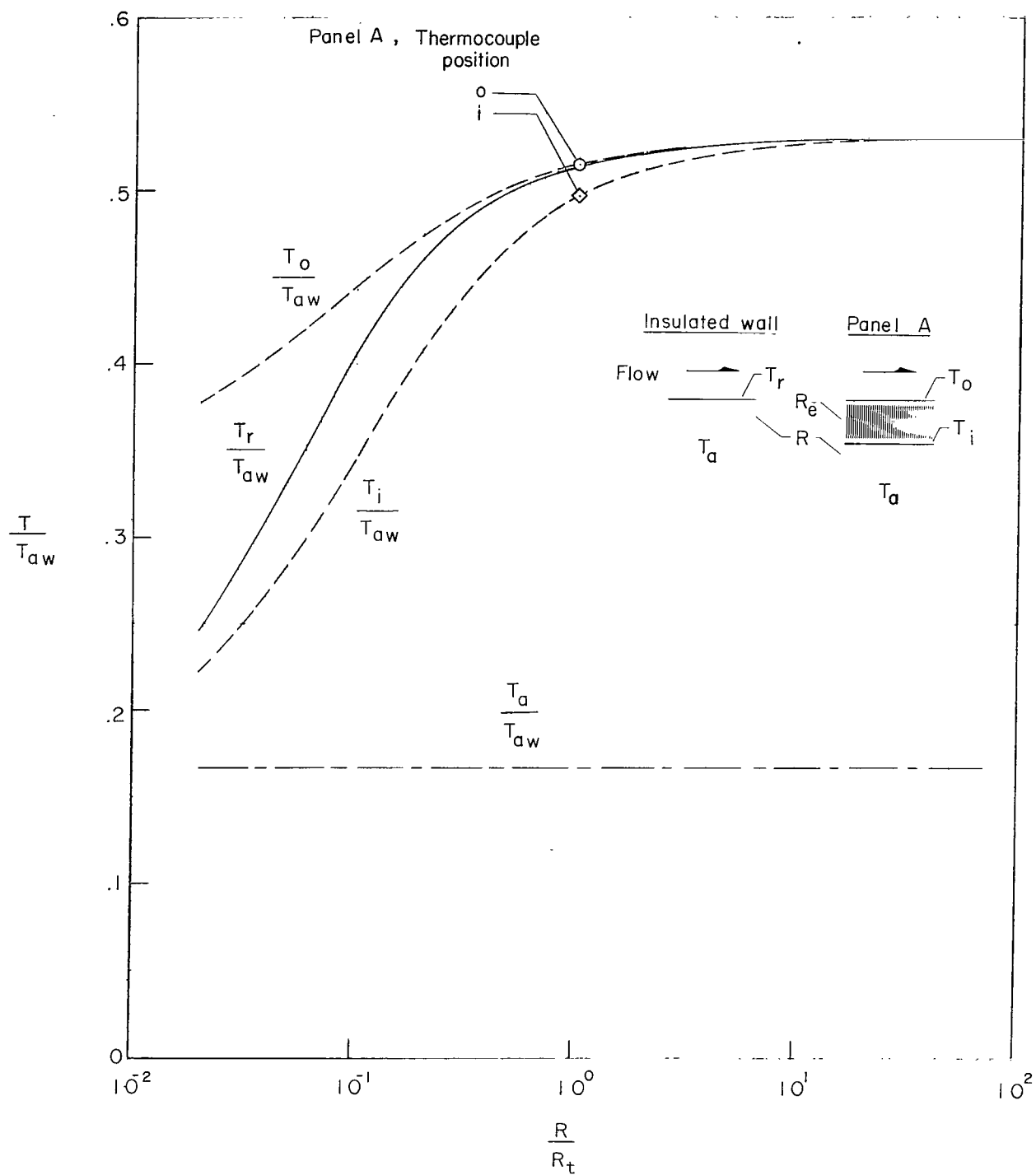
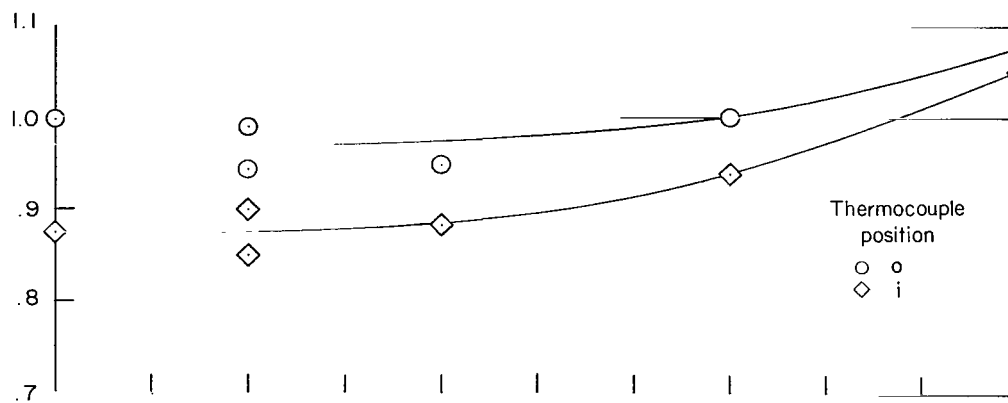
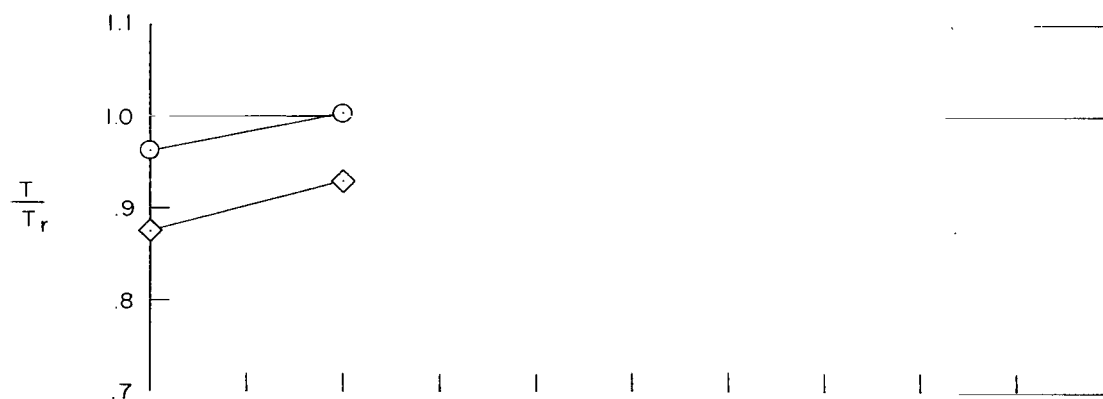


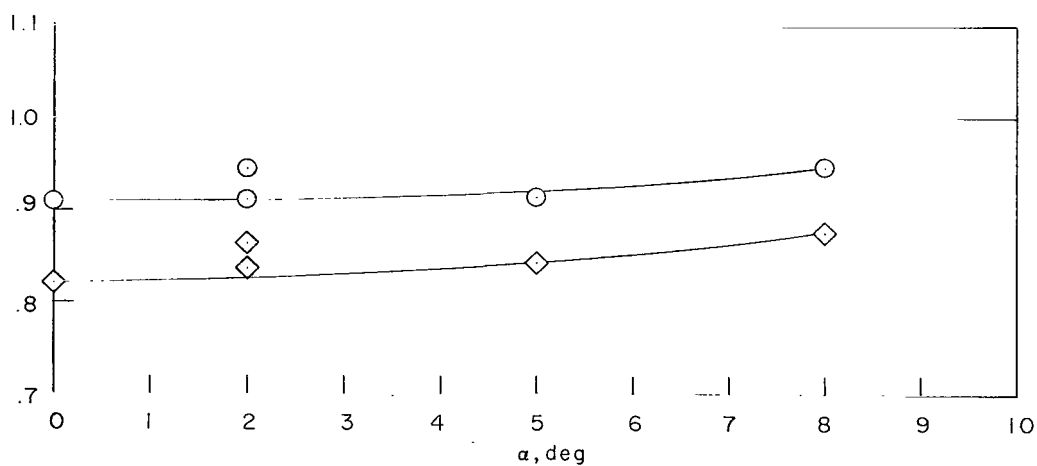
Figure 5.- Effect of insulation on steady-state wall temperature.  $T_{aw} = 3000^{\circ} \text{R}$  ( $1670^{\circ} \text{K}$ );  $h = 0.0011 \text{ Btu/ft}^2\text{-sec-}^{\circ}\text{R}$  ( $22.5 \text{ W/m}^2\text{-}^{\circ}\text{K}$ );  $\epsilon = 0.51$ ;  $R_t = 5000 \text{ ft}^2\text{-sec-}^{\circ}\text{R/Btu}$  ( $0.245 \text{ m}^2\text{-}^{\circ}\text{K/W}$ );  $R_e/R_t = 0.0555$ .



(a) Panel B.



(b) Panel C.



(c) Panel D.

Figure 6.- Variation of  $T/T_r$  for inner and outer surfaces of open-face honeycomb panels with angle of attack.

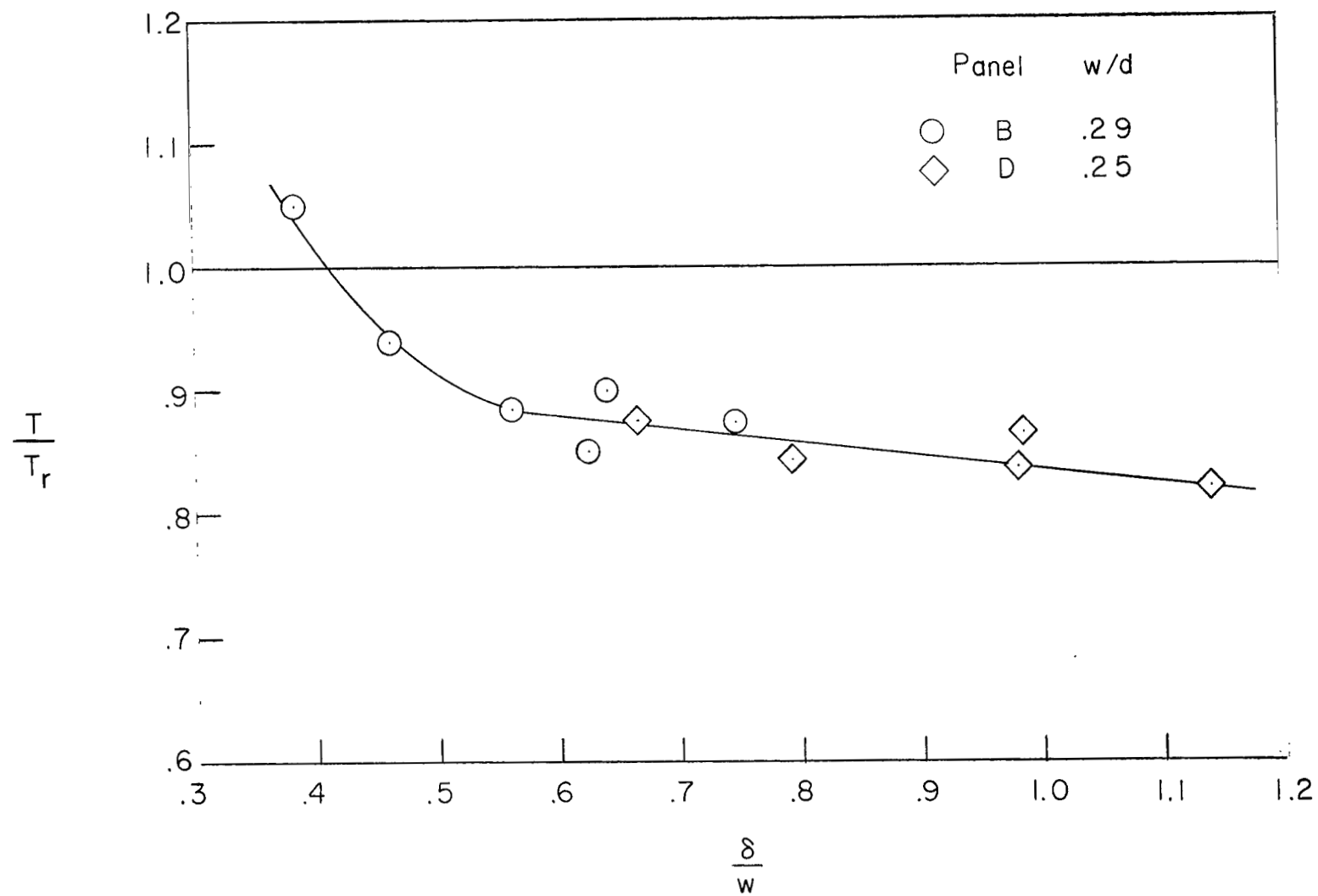


Figure 7.- Variation of  $T/T_r$  with ratio of boundary-layer thickness to cell width for open-face honeycomb panels of cell widths of 3/16 and 1/8 inch (4.8 and 3.2 mm).



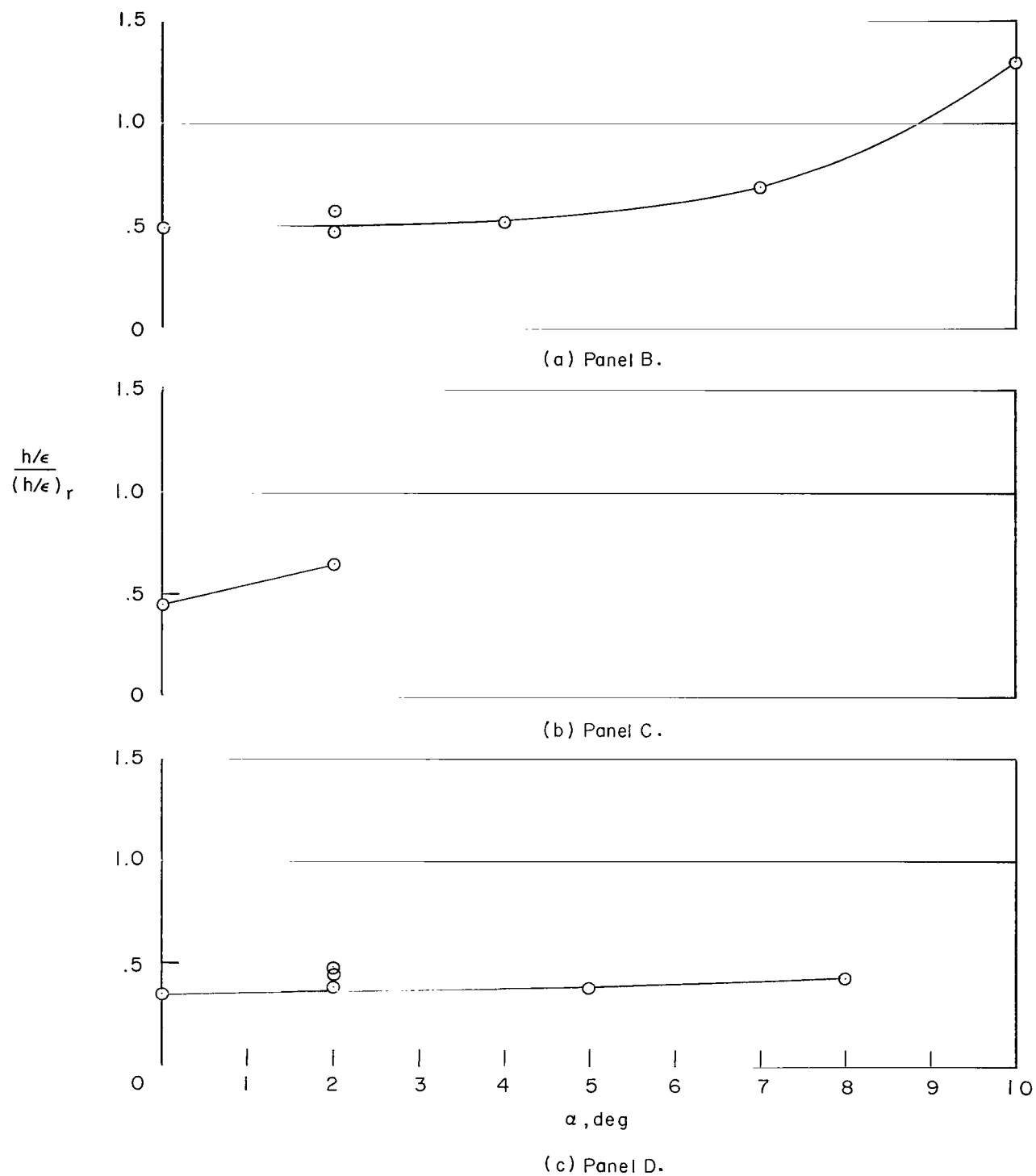


Figure 8.- Variation of  $\frac{h/\epsilon}{(h/\epsilon)_r}$  with angle of attack for the open-face honeycomb panels.

OFFICIAL BUSINESS

04-01-2014 14:35:00 01/03/2014  
 04-01-2014 14:35:00 01/03/2014  
 04-01-2014 14:35:00 01/03/2014

*"The aeronautical and space activities of the United States shall be conducted so as to contribute . . . to the expansion of human knowledge of phenomena in the atmosphere and space. The Administration shall provide for the widest practicable and appropriate dissemination of information concerning its activities and the results thereof."*

NASA SCIENTIFIC AND TECHNICAL PUBLICATIONS

**TECHNOLOGY UTILIZATION PUBLICATIONS:** Information on technology used by NASA that may be of particular interest in commercial and other non-aerospace applications. Publications include Tech Briefs, Technology Utilization Reports and Notes, and Technology Surveys.

SCIENTIFIC AND TECHNICAL INFORMATION DIVISION  
NATIONAL AERONAUTICS AND SPACE ADMINISTRATION  
Washington, D.C. 20546